AD-A092 565 PHILIPS LABS BRIARCLIFF MANOR NY F/G 17/5
OPTIMIZED PYROELECTRIC VIDICON THERMAL IMAGER. VOLUME I. THERMA--ETC(U)
JUN 79 R KURCZEWSKI, E STUPP, P MURAU DAAG53-76-C-0053
UNCLASSIFIED NL

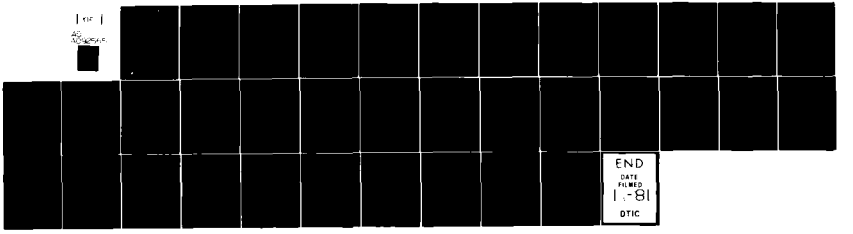

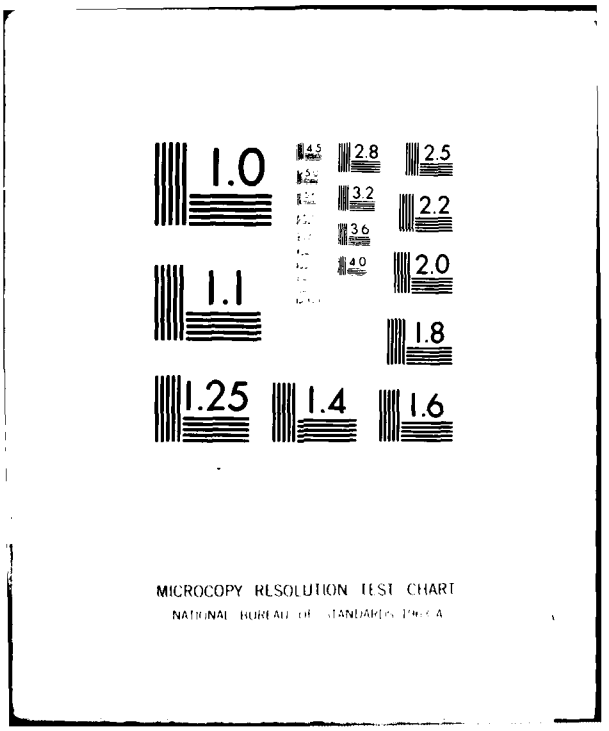
1.0
1.1
1.25
1.4
1.6
1.8
2.0
2.2
2.5
2.8
3.2
3.6
4.0
4.5
MICROCOPY RESOLUTION TEST CHART
NATIONAL BUREAU OF STANDARDS 1963-A

LEVEL III

OPTIMIZED PYROELECTRIC VIDICON THERMAL IMAGER
VOL. I: THERMAL IMAGER

SUPPLEMENT TO
FINAL TECHNICAL REPORT

7 June 1978 - 14 April 1979

VOL. 1a: RAIN CAMERA

by

R. Kurczewski
E. Stupp

VOL. 1b: RETICULATION

by

P. Murau
B. Singer

June 1979

Prepared for

NIGHT VISION & ELECTRO-OPTICS LABORATORY
USAECOM
Fort Belvoir, Virginia

Contract No. DAAG53-76-C-0053 (Mod. P00005)

Prepared by

PHILIPS LABORATORIES
A Division of North American Philips Corporation
Briarcliff Manor, New York 10510

UNCLASSIFIED

SECURITY CLASSIFICATION OF THIS PAGE (When Data Entered)

REPORT DOCUMENTATION PAGE

READ INSTRUCTIONS BEFORE COMPLETING FORM

1. REPORT NUMBER	2. GOVT ACCESSION NO. AD-A092
3. RECIPIENT'S CATALOG NUMBER	565 (9)
4. TITLE (and Subtitle) (6) Volume I: OPTIMIZED PYROELECTRIC VIDICON THERMAL IMAGER. VOL. I: THERMAL IMAGER. SUPPLEMENT TO FINAL TECHNICAL REPORT. VOL. Ia: RAIN CAMERA. VOL. Ib: RETICULATION.	5. TYPE OF REPORT & PERIOD COVERED: Supplement to Final Report, 7 June 1978 — 14 April 1979
	6. PERFORMING ORG. REPORT NUMBER
7. AUTHOR(s) (10) R. Kurczewski, E. Stupp, P. Murau, B. Singer	8. CONTRACT OR GRANT NUMBER(s) (15) DAAG53-76-C-0053 (Mod. P00005)
9. PERFORMING ORGANIZATION NAME AND ADDRESS: PHILIPS LABORATORIES, A Division of North American Philips Corp., Briarcliff Manor, New York 10510	10. PROGRAM ELEMENT, PROJECT, TASK AREA & WORK UNIT NUMBERS
11. CONTROLLING OFFICE NAME AND ADDRESS: Night Vision & Electro-Optics Laboratory, USAECOM, Ft. Belvoir, Virginia	12. REPORT DATE (11) June 1979
	13. NUMBER OF PAGES: 37
14. MONITORING AGENCY NAME & ADDRESS (if different from Controlling Office) (12) 36	15. SECURITY CLASS. (of this report): UNCLASSIFIED
	15a. DECLASSIFICATION/DOWNGRADING SCHEDULE

16. DISTRIBUTION STATEMENT (of this Report)

DISTRIBUTION STATEMENT A
Approved for public release;
Distribution Unlimited

17. DISTRIBUTION STATEMENT (of the abstract entered in Block 20, if different from Report)

18. SUPPLEMENTARY NOTES

19. KEY WORDS (Continue on reverse side if necessary and identify by block number)

Pyroelectric vidicon
Thermal imaging
Reticulated targets
Pedestal noise suppression
DTGS
DTGFB

20. ABSTRACT (Continue on reverse side if necessary and identify by block number)

A technique for suppressing the noise resulting from pedestal generation in the pyroelectric vidicon has been developed. System modifications were implemented to provide reduced bandwidth and line rates in order to effect a factor of four bandwidth reduction. Under these conditions, the pedestal noise is completely dominant. Implementation of the pedestal noise suppression technique then results in a factor between three and four improvement in the MRT's. Performance of the chopped-mode system is close to the best performance reported for the pan mode.

(Continued) over

DD FORM 1 JAN 73 1473 EDITION OF 1 NOV 65 IS OBSOLETE

387334 A

UNCLASSIFIED

SECURITY CLASSIFICATION OF THIS PAGE (When Data Entered)

20. ABSTRACT (Continued)

Reticulation of the TGS family of pyroelectric targets was demonstrated using standard ion-milling techniques. Reticulation of DTGFB was successfully demonstrated by reactive ion milling using aluminum as a mask. The optimum depth achieved in the latter case was 18-20 micrometers, which translates into an aspect ratio of about 4:1. Both reticulated DTGS and DTGFB target were successfully constructed wherein individual dice were completely isolated from neighboring dice such that thermal spread was minimized. Several PEVs with reticulated targets were evaluated which indicate significant improvement in performance of DTGS targets and some modest improvement of DTGFB targets over single crystal targets. The optimum effect of reticulation at high spatial frequencies has been realized with DTGS targets but not yet with DTGFB targets.

1473 B

SUMMARY

A technique for suppressing the noise resulting from pedestal generation in the pyroelectric vidicon has been developed. System modifications were implemented to provide reduced bandwidth and line rates in order to effect a factor of four bandwidth reduction. Under these conditions, the pedestal noise is completely dominant. Implementation of the pedestal noise suppression technique then results in a factor between three and four improvement in the MRT's. Performance of the chopped-mode system is close to the best performance reported for the pan mode.

Reticulation of the TGS family of pyroelectric targets was demonstrated using standard ion-milling techniques. Reticulation of DTGFB was successfully demonstrated by reactive ion milling using aluminum as a mask. The optimum depth achieved in the latter case was 18-20 μm, which translates into an aspect ratio of about 4:1. Both reticulated DTGS and DTGFB target were successfully constructed wherein individual dice were completely isolated from neighboring dice such that thermal spread was minimized. Several PEVs with reticulated targets were evaluated which indicate significant improvement in performance of DTGS targets and some modest improvement of DTGFB targets over single crystal targets. The optimum effect of reticulation at high spatial frequencies has been realized with DTGS targets but not yet with DTGFB targets.

PREFACE

This work was performed by Philips Laboratories, a Division of North American Philips Corporation, Briarcliff Manor, New York under the overall supervision of Dr. Barry Singer, Director, Component and Device Research Group. Mr. Richard Kurczewski was Program Leader for the camera system modifications and demonstrations; Dr. E. Stupp, Senior Program Leader for Solid State Components, was available in a consulting and advisory capacity. Upon Mr. Kurczewski's transfer to another Philips company, the Magnavox Government and Industrial Electronics Corporation, Mahwah, N. J., the remainder of the rain camera task was subcontracted to that organization. Mr. Peter Murau was responsbile for the reticulation effort.

The program was issued by the U.S. Army Mobility Equipment Research and Development Center, Fort Belvoir, Virginia, and was initiated under Contract DAAG53-76-C-0053. Mr. Ferdinand Petito was the initial Contracting Officer's Representative for the Night Vision and Electro-Optics Laboratory, USAECOM; Dr. Lynn Garn served in this capacity in the later phases.

The work described in this Final Technical Report covers the period from 7 June 1978 - 14 April 1979.

TABLE OF CONTENTS

LIST OF ILLUSTRATIONS

VOLUME 1a: RAIN CAMERA

1. INTRODUCTION

In measuring and demonstrating the performance of an Optimized Pyroelectric Vidicon Thermal Imager under Contract No. DAAG53-76-C-0053 funded by Night Vision & Electro-Optics Laboratory, Fort Belvoir, Virginia, it was evident that present pyroelectric vidicon (PEV) systems have highly satisfactory performance for many applications. However, when these PEV systems were considered for certain mission applications, the signal-to-noise ratio in the display $(S/N)_D$ was found to be inadequate under low contrast conditions, such as those resulting from a viewed scene exposed to a prolonged period of rain. This contract effort (Mod. P00005) was devoted to improving the $(S/N)_D$ under this type of adverse condition. Hence, this improved PEV camera has been called the "rain camera".

The performance of the pyroelectric vidicon is, like any video component, determined by the signal-to-noise ratio. An increase of signal or a reduction of the noise results in improved system performance. Significant efforts had been expended in the past to successfully increase the S/N by increasing the signal levels.[1] This program was intended to demonstrate the S/N improvements which result from reducing the system noise.

The noise in PEV systems is primarily caused by pedestal generation and by the preamplifier. It has been shown[2] that the pedestal and preamplifier noise are comparable for a system bandwidth of 5 MHz ($i_{ped} \simeq i_{PA} \simeq 1$ nA). Implementation of any noise reduction technique which addresses only one of these noise sources cannot reduce the overall noise by more than about 40% for the same system bandwidth.

---

(1) See, e.g., Final Report, Contract DAAG53-75-C-0256, August 1976.

(2) Contract DAAK70-77-C-0138, Progress Report May 1978.

A technique for pedestal noise suppression (PNS) is being investigated as part of Contract DAAK70-77-C-0138 (Return Beam/Isocon Pyroelectric Thermal Imager). In this effort, the internal noise sources are made dominant over the preamp noise by use of internal gain in the tube. PNS would then permit reduction of system noise for a signficant S/N improvement. The program reported here demonstrates significant S/N improvements in PEV systems by simultaneously reducing preamp noise via bandwidth reduction and pedestal noise via PNS. Bandwidth reduction without resolution loss is accomplished with reduced beam scanning rates.

2. PEDESTAL GENERATION AND NOISE

The magnitude of pedestal noise depends upon the means of pedestal generation, and it is lowest in the secondary emission pedestal mode (SEPM).[3] In this method, positive charge is generated on the target during the system's horizontal flyback period. Consider a horizontal line of a raster as shown in Figure 1. The positive charge is generated on the target by reducing the cathode potential to -80 V during flyback (instead of leaving it at 0 V). This causes electrons to strike the target with 80 eV of energy.

The secondary emission coefficient for an 80 V primary electron is about two (2), i.e, two electrons will leave the target and be collected by the mesh for each primary electron that lands. The charge thus created on the target is the positive pedestal charge and that charge, readout in one field time, is the pedestal current. Unfortunately this pedestal current is not noiseless. The sources of the noise are the primary electron beam striking the target and fluctuations in the secondary electron emission coefficient.

---

(3) B. Singer, "Theory and Performance Characteristics of Pyroelectric Imaging Tubes", in Advances in Image Pick-up and Display, B. Kazan, ed., Academic Press, 1977.

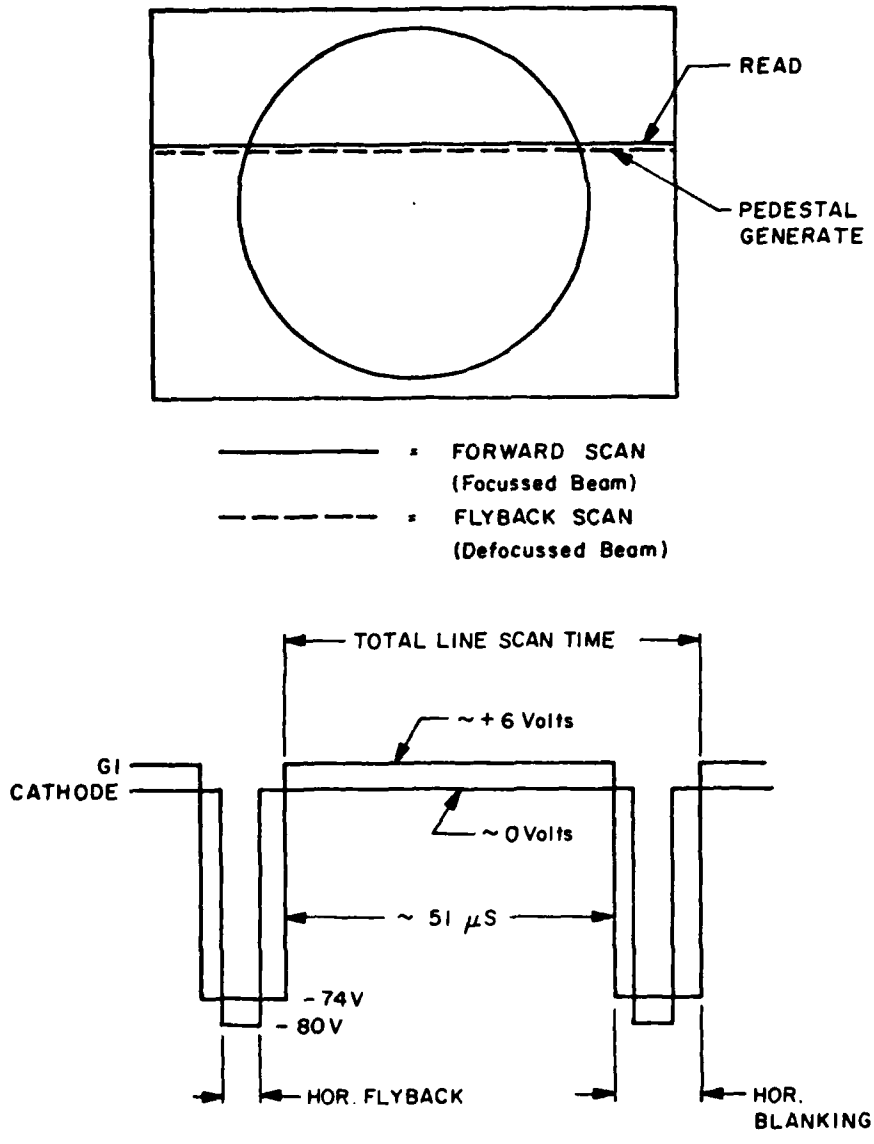

Figure 1. Scan sequence and electrode potentials for standard SEPM operation of the PEV.

In addition to the random noise, there is nonuniformity in the pedestal of about 10-20%, which degrades the picture quality. In practice, about 100 nA of pedestal current is used and this results in about 10-20 nA nonuniformity. When we consider that a typical pyroelectric signal is 1-2 nA, this nonuniformity can be quite serious in determining the overall image quality.

3. REDUCTION OF PEDESTAL NOISE AND NONUNIFORMITY

The pedestal noise and nonuniformity may be greatly reduced as illustrated in Figure 2, where an augmented SEPM is shown. The forward scan (Fig. 2a) is the same as in the SEPM. The information and pedestal is read during this time as the beam goes from 1 to 2. During the blanking interval the beam goes from 2 to 3,

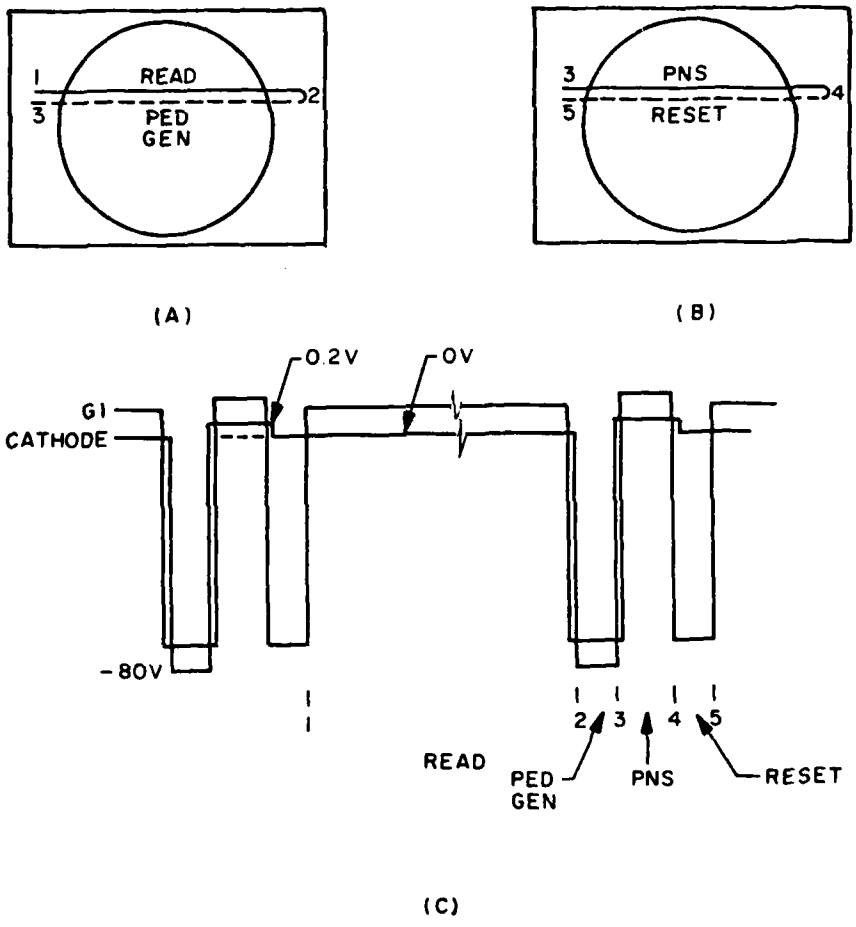

Figure 2. Modified scan sequence and electrode potentials for pedestal generation and pedestal noise suppression.

and pedestal is generated by pulsing the cathode to -80 V (Fig. 2c) and knocking out secondaries, as usual. However, if 100 nA of pedestal current is now required, an excess is put down, e.g., 200 nA. Then the beam again scans over the same flyback line from 3 to 4 (Fig. 2b). Now, however, the cathode is at

a potential V_c, shown in Figure 2c to be 0.2 V positive. As the beam scans over the free surface of the target during the period called flyback read, it charges the free surface down to a potential V_p above the quiescent value as shown schematically in Figure 3.

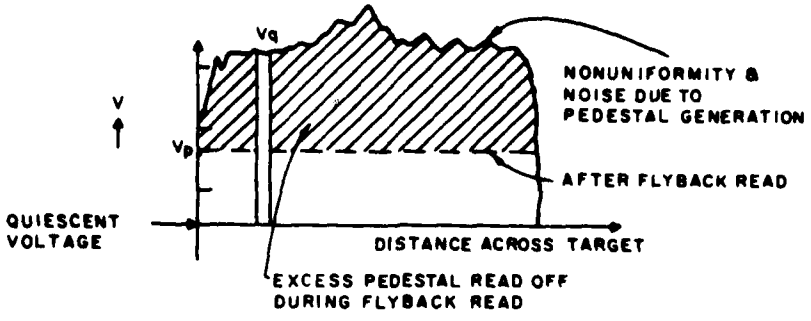

Figure 3. Schematic illustration of free surface potentials along one horizontal line. V_s is reached after read, V_q after pedestal generate, and V_p after PNS.

Since the beam tends to read the pedestal level to a fixed value above the quiescent value, most of the nonuniformity and noise is suppressed. Assuming that the efficiency in readout is high, the noise remaining is only that from the read beam. The system is then reset, going from 4 to 5 with the beam blanked off, as in a normal vidicon, and it starts to read another line.

4. IMPLEMENTATION OF PEDESTAL NOISE CLEAN-UP

The key to reducing pedestal noise and nonuniformity is to generate and "clean-up" the pedestal on the same flyback line immediately behind the forward readout line. Previous experience indicated that pedestal was generated during flyback scan at an angle to the normal (forward) scan line.[4] During pedestal generation, the electron beam is defocussed as a result of pulsing the cathode and G1. The defocussed electron beam travels a different path during flyback than that of the

(4) Contract No. DAAK70-77-C-0138, Progress Report July 1977.

focussed beam during forward scan. Laboratory measurements indicated that pedestal generation occurs at a 7° to 8° angle with respect to the normal scan. The pedestal generating beam was defocussed to a width of 10 TV lines and was displaced $\pm$ 20 TV lines around a reference scan line. Figure 4 schematically depicts the normal and pedestal generating scans.

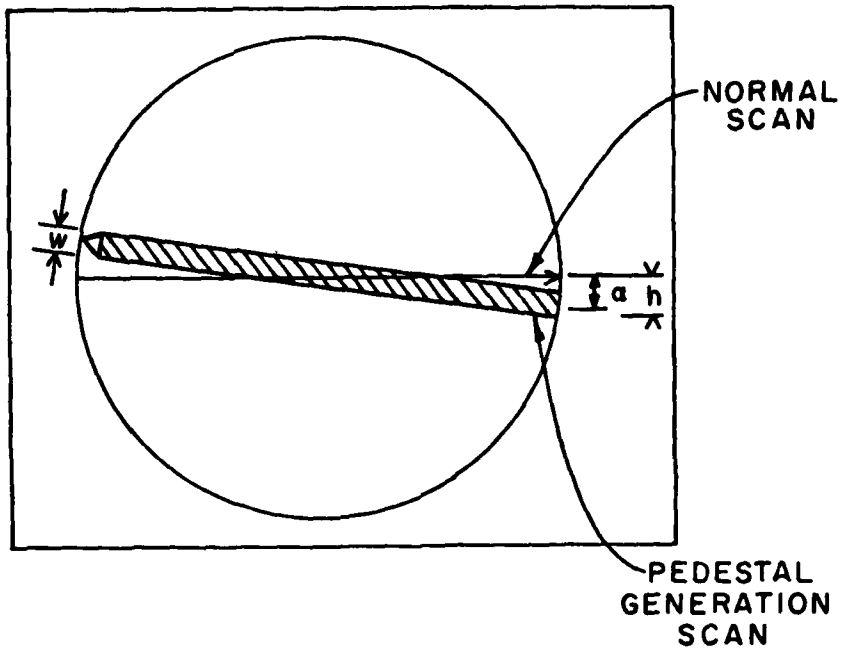

Figure 4. Rotation and defocusing of pedestal generation scan. Angle α is about 7.5°, defocus width W is about 10 TVL, and maximum deviation h of pedestal from normal scan is 20 TVL.

The PNS beam is parallel to a normal forward scan line since the electrode potentials are essentially the same as in the normal scan. The rotated pedestal generating beam would generate noise and nonuniformity in areas just ahead of the readout beam on one side of the target. To avoid this, the pedestal generating and noise suppression scans are kept in focus and parallel to the forward scan lines. Focus of the electron beam is controlled by pulsing the G3 (drift tube) electrode in the vidicon.

It is evident from the description of the pedestal noise clean-up scheme that the standard/normal horizontal flyback must be modified into three sweeps. The three flyback time periods are identified as:

(A) pedestal generation
(B) PNS
(C) beam return (reset).

Figure 5 illustrates how a standard 63.5 μs horizontal period can be divided into the required forward and flyback scans.

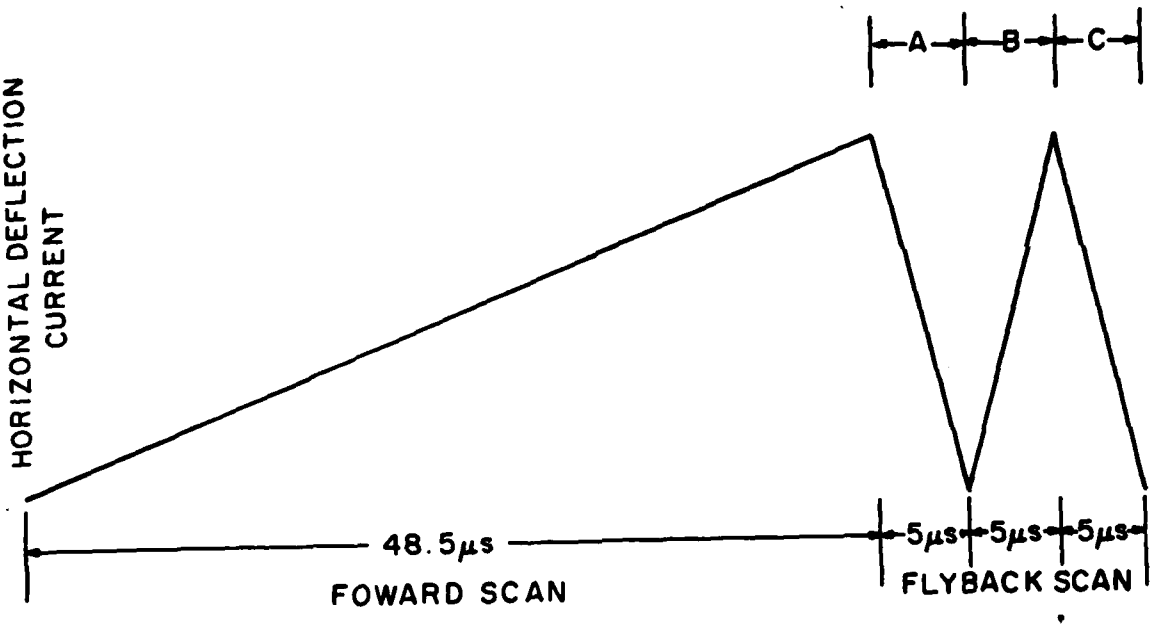

Figure 5. Sweep waveform for pedestal generation and noise reduction.

The linear deflections during the A, B and C flybacks impose severe driver requirements which cannot be met by standard camera deflection circuitry. A Celco deflection amplifier and low-impedance deflection yoke were used in the "rain camera".

To insure that the pedestal generation and noise suppression scans fall behind the forward (normal) scan, it is required to dither the vertical deflection. A standard PEV raster of 4:3 aspect ratio uses about 51 μs for the forward scan. About 10 μs of the forward scan is spent "off the target". This "off target" time is uses as additional flyback time for clean-up. Figure 6 shows the resulting 7.8 μs flyback scans and 40 μs forward scan when using a 1:1 aspect ratio. The horizontal and vertical deflection currents are shown in Figure 6b. Detail "A" of the vertical deflection depicts the requirement to dither the flyback beam.

A XEDAR camera was modified for demonstrating pedestal noise suppression. The modifications included cathode and G1 control for pedestal generation, G3 pulsing for focus, timing and waveshape generation for deflection control, and mechanically installing the Celco deflection amplifiers and yoke.

When the pedestal noise suppression circuitry was made operational, it was found that the "clean-up" resulted in non-uniform reduction of pedestal current across the tube. The non-uniformity was very dependent on the current settings of the beam alignment coils. It was apparent to the observer that the PNS circuitry reduced the fixed pattern noise in local regions. However, the pedestal shading resulting from the non-uniform pedestal reduction had to be eliminated if the benefits of noise reduction were to be obtained.

During investigation of the sources of non-uniform pedestal suppression, several observations were made which led to a rather extensive redesign of the PNS circuitry. With the pedestal generate and pedestal clean-up beams in focus, and equal amplitudes of the horizontal deflection current for the generate (A) and clean-up (B) flybacks, and forward/normal scan, the following observation were made:

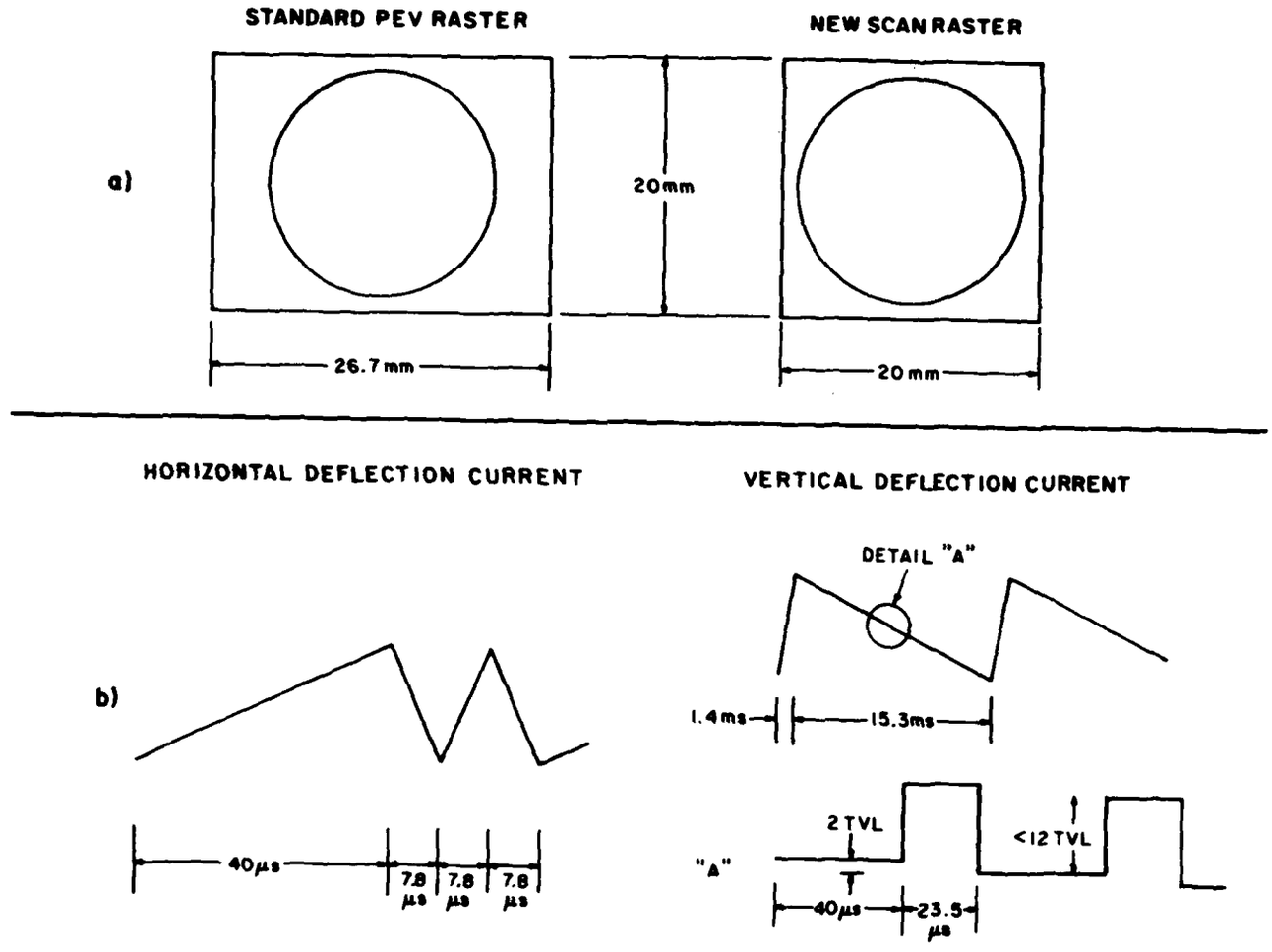

Figure 6. (a) Rasters used for a standard PEV and for a PEV with pedestal noise suppression. (b) Deflection current waveforms for new scan raster.

- Pedestal generation did not cover the whole target.
- Pedestal clean-up did not coincide with pedestal generate and also did not cover the whole target.
- With the same vertical dither (step-back) for both flyback periods, the pedestal clean-up line was displaced from the pedestal generate line.

These results are due to the magnetic deflection employed in the PEV. The rapid pulsing of the deflection coils gives rise to eddy currents in the G3 electrode of the tube, resulting in nonlinear scans. The current pulses to the coils can capacitatively coupled through the coil without generating the expected magnetic fields. Some of the steps taken to minimize these problems were:

- Slotted drift tube in the PEV to reduce eddy currents.
- Tilt and step compensation in the deflection circuitry.
- Separate beam focus control during forward scan, generate, and clean-up scan times.
- Instituting slow-scan to take advantage of longer horizontal flayback times.

5. SLOW SCANS AND PNS

The primary causes of the non-uniform pedestal noise suppression are nonlinear scans resulting from capacitive feedthrough of the deflection pulses through the coil and eddy currents. These nonlinearities resulted in positional, dwell-time, and beam alignment errors in pedestal generation and suppression. Since the rain camera was intended to operate at reduced line and frame rates (for preamp noise reduction), the camera was modified at this time to slow down the scans. This would minimize the nonlinearities for the PNS demonstration.

The camera system was changed from the standard 525 lines, 60 Hz field rate of conventional TV systems. Two slow-scan modifications were performed. First, the scan rates were changed to 525 lines, 30 Hz field rate; then, the scans were changed to 263 lines, 30 Hz field rate, which are the proposed scan rates for the "rain camera".

Several special PEVs were fabricated for the PNS demonstrations. These tubes had slotted drift tubes to reduce eddy currents generated in this electrode by the rapidly changing horizontal and vertical deflection fields. The tubes also had larger limiting apertures (90 μm compared to the normal 60 μm) to provide more beam during the flyback read interval. A square mask of 18 μm diagonal was also used on the target in order to allow scan size and hence deflection currents to be limited, and to improve beam landing characteristics.

The reduced scan rates provided longer horizontal flyback time. This resulted in reduced deflection drive requirements, reduced eddy current generation, and additional time for the flyback read.

Coupled with the first scan rate reduction, the preamplifier bandwidth was reduced from 4 MHz to 2 MHz with the accompanied reduction of equivalent input noise current to 0.4×10^{-9} A rms.

At this point (October 1978), pedestal noise clean-up was qualitatively demonstrated, both on the video display and on a line-scope monitor. The video display showed PNS to be effective over about the central 80% of the target. The pedestal level was uniformly reduced in this area and defects, particularly white defects, were suppressed. The line-scope showed a reduced peak-to-peak noise amplitude with PNS. Noise was observed for a conventional 100 nA pedestal level and for a 100 nA level suppressed from 200 nA via the PNS circuitry. It is the latter situation which showed reduced peak-to-peak noise.

It should be moted that all performance and operational observations were done with the system in the chopper mode. The chopper control system was modified so that at the new 30 Hz field rate, the chopper operated at one field open, one field closed, i.e., 15 Hz.

6. PREAMPLIFIER

As previously noted, the unsuppressed pedestal noise and preamplifier noise are comparable. Implementation of PNS alone would result in a PA noise limited system with about only a 40% S/N improvement. The preamplifier noise current is given by:

$$\bar{i}_{PA} = \left[\frac{4kT}{R} + \frac{16}{3} \pi^2 kTR_n C^2 \Delta f^2 \right]^{1/2} \Delta f^{1/2}$$

where k = input resistance of amplifier, R_n = equivalent noise resistance of amplifier, and C = total capacitance across amplifier input.

The preamplifier noise can be reduced by bandwidth reduction. When the second term in the above expression is dominant, a factor of four reduction in bandwidth results in a factor of eight reduction in noise. Loss of high frequency information is avoided by reducing the information rate by halving both the field rate and number of horizontal scan lines.

Prior to these slow scan modifications, the camera preamplifier bandwidth was measured to be 5 MHz with an equivalent input noise current of 1.2×10^{-9} A rms. By changing the input resistance R of the amplifier from 1×10^5 ohms to 3×10^5 ohms and setting the appropriate compensation stages for a bandwidth of 4 MHz, the calculated noise becomes 0.77×10^{-9} A and was measured to be 0.8×10^{-9} A. Along with the first

slow scan modification (field rate reduction to 30 Hz), the preamplifier bandwidth was reduced from 4 MHz to 2 MHz with the accompanying reduction of equivalent input noise current to 0.4×10^{-9} A rms.

The second slow scan modification required a bandwidth reduction to 1 MHz. At 1 MHz bandwidth, the 3×10^{5} ohm input resistance is the predominant noise contributor. The input resistance was changed to 1 megohm along with the appropriate compensation adjustments and resulted in an equivalent input noise current of 0.2×10^{-9} A rms for a 1 MHz bandwidth. This noise compared favorably with the calculated noise of 0.15×10^{-9} A rms.

7. RAIN CAMERA PERFORMANCE

Despite all of the electronics changes made to obtain uniform reduction of the pedestal current across the target with PNS, non-uniformities remained. The degree of non-uniformity was very much beam-alignment-adjustment dependent. Nevertheless, in those areas where the reduction was uniform, the pedestal noise was significantly reduced.

To take advantage of the noise reduction, however, the non-uniformity had to be eliminated. The camera was connected to the Image Difference Processing (IDP) System to take advantage of the feature of IDP such as tube background cancellation. Indeed, IDP smoothed out the tube background and allowed the use of additional gain so that the system noise could be detected by the eye.

On 12 April 1979 the system was demonstrated and measured at NVEOL. The results of the MRT measurement for the "rain camera" are shown in Figure 7 along with the MRTs for a standard PEV camera system with IDP. The data was taken with a 50 mm lens at f/2 and extrapolated to f/0.7 with previously measured transmission data. The transmission of this lens at f/0.7 is only 1.5 times that at f/1 rather than the expected 2 times. The data presented reflects the actual lens transmission.

As shown in Figure 7 an improved performance by a factor of 3 to 4 was achieved by the rain camera.

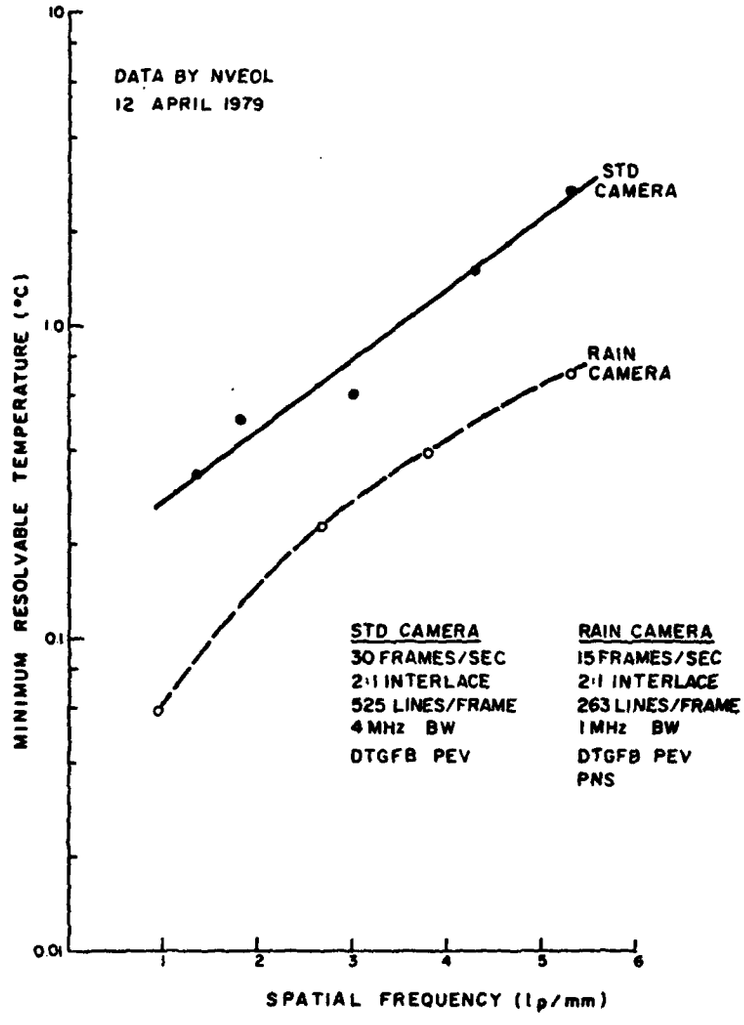

Figure 7. MRTS of standard DTGFB PEV system and rain camera as determined by NVEOL. The data was taken with a 50 mm lens at f/2 and extrapolated to f/0.7 with previously measured transmission data.

8. CONCLUSIONS

The MRTs obtained with a pyroelectric vidicon system have been dramatically reduced by implementation of pedestal noise suppression and slow-scan. The performance of this chopped-mode system is close to the best performance reported for the pan-mode.

While the principle of noise reduction was successfully demonstrated, system problems associated with the magnetic focus and deflection in this generation of PEVs would make a practical, physically-small system difficult to achieve. To avoid these difficulties, it is recommended that an all-electrostatic PEV be developed. With the present understanding of the pedestal-noise-suppressed PEV, it is believed this development would permit a small, chopped-mode PEV system to be built having performance suitable for several dedicated mission applications, including those requiring operation under adverse signal conditions.

VOLUME 1b: RETICULATION

1. INTRODUCTION

The objective of the thermal imager portion of Philips Laboratories program under Contract No. DAAG53-76-C-0053 was to obtain an overall system performance of an MRT of 0.2°C at a limiting resolution of 350 TV lines with f/0.7 optics. It was anticipated that this performance could be achieved by the use of a pyroelectric vidicon image tube with a target of reticulated DTGFB. Candidate target materials, as defined by the Purchase Description of subject contract, were to be TGS, TGFB and DTGFB, with the added proviso that the materials would "only be required after they became available in industry..."

At the time of the March 1977 review with the Contracting Officers Technical Representative, PL had successfully fabricated reticulated TGS tubes, demonstrated performance which closely approached the theoretical prediction, and anticipated meeting all obligations of the contract. Difficulaties developed, however, when that reticulation technology was applied to TGFB and DTGFB targets. Modification P00005 was issued to cover identification and experimental verification of the problems associated with reticulating TGFB and DTGFB material.

2. RETICULATION TECHNOLOGY

TGS material was used for the reticulation studies under the basic contract because TGFB and DTGFB were not available in sufficient quantities during the early part of the program. The three techniques investigated were: ion beam milling, wet chemistry etching, and plasma etching. Ion beam milling was the first technique eliminated because the resultant target structure had reticulated dice with very steep walls, and it was not possible to generate pedestal because the electron beam charged the dice walls negatively. This prevented any further landing of the electron beam. The wet chemistry process appeared to be quite cumbersome and not suitable for reasonable yield and good cosmetic quality of the targets. Plasma etching produced

targets of suitable geometry, and TGS reticulated targets were fabricated by this technique and evaluated in tubes. The performance was very close to theoretical predictions.

When the plasma reticulation technology was applied to TGFB and DTGFB targets, however, the following results were obtained:

- Cosmetic quality was good although there was evidence of fixed pattern noise.
- Sensitivity at low spatial frequencies was less than that of single-crystal, non-reticulated material.
- Sensitivity at high spatial frequencies was poor. Tubes were laggy.

A microscopic examination of the target geometry revealed a significantly different morphology than with TGS. This resulted in a much greater kerf loss and had the effect of making target thickness equal to the thickness of the residual material left in the valleys.

Two distinct problem areas were identified and experimentally confirmed. First, there was the problem associated with beam landing on the non-planar surface of the reticulated TGFB and DTGFB structure. The resulting poor beam acceptance gave an effective high beam impedance and, when coupled with the large kerf loss, was responsible for the lag and the poor performance at high spatial frequencies. Further, fixed pattern noise also resulted from the beam landing on the non-planar surface. When the target was reversed so that the substrate was addressed by the beam, the fixed pattern noise was practically eliminated. Second, it was verified that the loss of sensitivity at low spatial frequency was due to material damage during the plasma etching.

3. ION MILLING

While the early ion-milled targets did not work, application of subsequently developed, bonding substrate technology to ion-milled targets appeared extremely promising. It was experimentally determined that one can satisfactorily operate an ion-beam-machined, reticulated TGS target when both sides of the retciulated target are covered by Pyre-ML films. The electron beam sees a planar surface and is prevented from charging the dice walls negatively. The performance of a TGS target fabricated by the above technique was as good as single-crystal target performance in the demount camera.

Based on the above, it was decided that the most promising technology for reticulating DTGFB is the modified ion-milling approach and that this should be pursued in a well-defined manner. The optimum structure should have minimum kerf loss, damage-free material, and planar surfaces for electron beam addressing. It was expected that structures of ion-beam-machined DTGFB islands, sandwiched between two layers of Pyre-ML and coated with an appropriate electrode (Sb) and a protective (SiOx) film, would satisfy the necessary criteria for a high-performance, pyroelectric target.

4. RESULTS

Three reticulated tubes were delivered under the contract, viz., two DTGFB and one DTGS. The DTGS tube was excess to the contract commitment. While data sheets and target processing procedures follow (see Fig. 1), some supplementary information is in order.

The DTGFB tubes performed well and showed a slight MTF improvement over conventional single-crystal DTGFB tubes. Full performance was not achieved, however, because the tubes are not fully reticulated but, rather, have about 11-12 μm reticulation with 3-4 μm of valley. Further, they showed cosmetic defects which were mainly black spots picked up in transit between

PL and Long Island where the ion-milling was performed. The DTGS tube, however, is reticulated throughout and has no valleys. It does, however, lack cosmetic quality.

Subsequently, an in-house, ion-beam-miller was received and made operational and a series of DTGFB and DTGS targets fabricated. The tubes made from these targets showed improved cosmetic quality and also improved performance. Although we were able to make a DTGFB tube which showed a significant improvement in contrast transfer function (CTF) (Fig. 2), we were not able to achieve the full potential, which should be about 2 nA°C at 5 lp/mm. We actually achieved a 1.1 nA/°C at that spatial frequency, an improvement of 1.5 in signal. On the other hand, with DTGS we were able to achieve a full factor of 3 improvement in performance at 5 lp/mm and a factor of 2 at 2.5 lp/mm. We believe the reason for not achieving the full potential with DTGFB was the use of aluminum during the ion-beam-milling procedure. We now believe the aluminum has to be etched-off completely before the Pyre-ML layer is put on.

Figures 2 and 3 give the sensitivity versus spatial frequency and CTF of recently made, reticulated DTGS tubes. Figures 4 and 5 give the corresponding results for the DTGFB tubes. Table 1 below gives ion-milling information for DTGS, DTGFB and masking materials used in the reticulation process. Work will continue at PL, at a low level of effort, on reticulated DTGFB and DTGS tubes to refine the process, improve the cosmetic quality, and achieve the full potential inherent in the DTGFB material.

TABLE 1. Ion Milling Rates (μm/min).

	O_2		Ar	
	500 V	1000 V	500 V	1000 V
PHOTO RESIST	0.15	0.20	0.06	0.08
ALUMINUM	<0.01	0.01	0.02	0.11
DTGFB	0.10	0.35	0.10	0.48
DTGS	1.2	4.3	0.80	3.1

SUBSTRATE TILT- 45°
CHAMBER PRESSURE -2×10^{-4} TORR

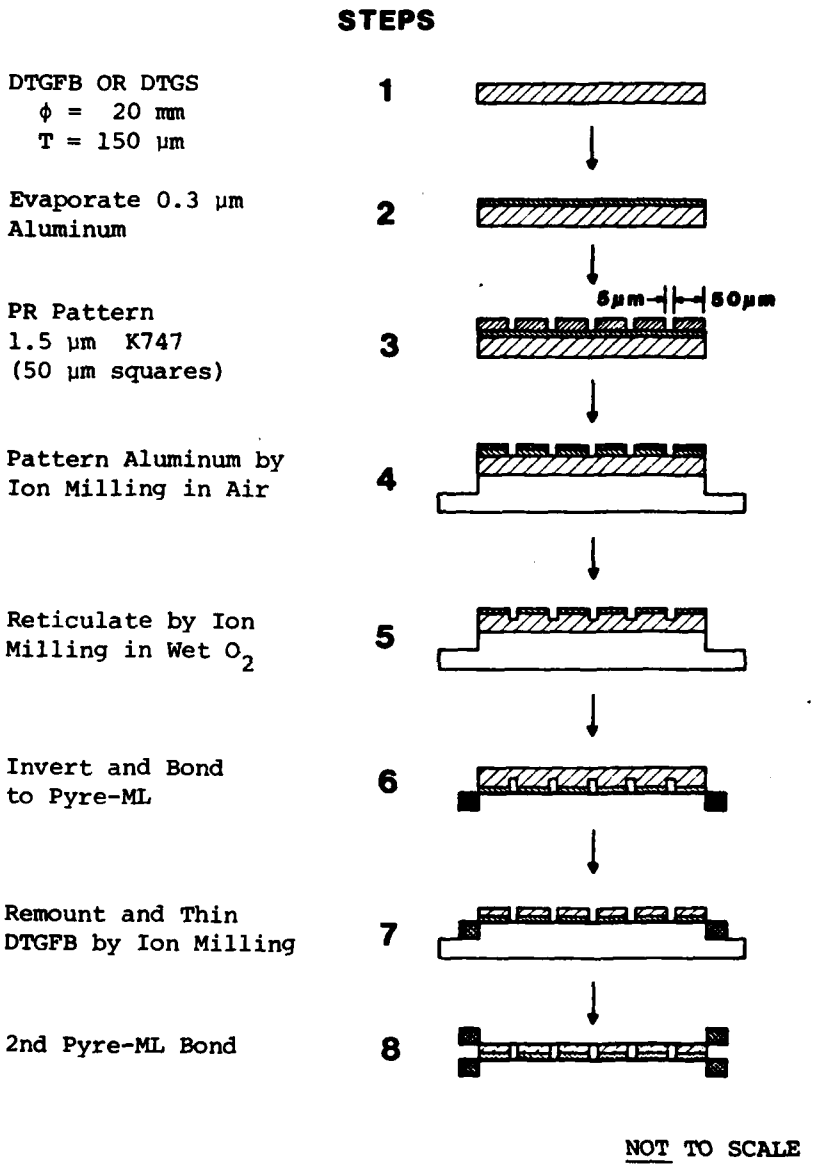

Figure 1. Fabrication sequence of a reticulated PEV target.

(Sheet 1 of 2)

SUMMARY OF RETICULATED TARGET FABRICATION PROCESS

(1) Targets are covered with aluminum about 0.3 μm thick and mounted on a copper block.

(2) Photoresist is spun on target and aluminum patterned by developing photoresist, then using wet chemical means. Or, on some targets, a more satisfactory practice was established to pattern the aluminum; this is accomplished by developing the photoresist, then using the ion beam miller with argon gas to pattern the aluminum.

(3) Target is then ion beam milled for a period of about one hour. DTGFB and TGFB are milled in a wet oxygen gas mixture while DTGS targets are milled in argon.

(4) Targets receive a layer of Pyre-ML and are removed from copper block and cup-etched down to a thickness of about 30 μm.

(5) Targets are then put back on block (reticulated side toward block) to remove the 15-20 μm of unreticulated material.

(6) Targets are then removed from block a second time and second Pyre-ML layer is put on.

(7) Target receives its normal processing SiO_x, antimony, mounting on Ge faceplate, etc.

Figure 1. Fabrication sequence of a reticulated PEV target.

(Sheet 2 of 2)

PHILIPS LABORATORIES
DATA SHEET

PEV No.: 325
Gun No.: 42395
Target : DTGS, reticulated

ELECTRICAL

Filament	6.3 V
G_2/G_3	280 V
G_4	450 V
Target	- 10 V
Auxiliary Heater(1)	5 V
Alignment(2)	
G_1 Forward	7 V
Cathode Forward	
G_1 Reverse(3)	
Cathode Reverse(3)	

PERFORMANCE*

Lag(1) $\alpha = I/I_o = e^{-\beta} = 0.5$

$I_{pedestal} = 75$ nA

* Scan 3:4 aspect ratio, 20 mm scan height.

	TVL/PH				
	10	50	100	150	200
Sensitivity(4) (nA/°C)	1.44	1.4	1.2	---	1.1
Contrast Transfer	1	0.97	0.83	---	0.76

Notes:

(1) Heater voltage set to achieve low spatial frequency sensitivity of 1.44 nA/°C. Volts may vary with camera conditions. Lag measured at S = 1.44 nA/°C.

(2) Alignment currents using Philips MP camera vidicon deflection coil.

(3) G_1 reverse is pulse voltage for pedestal generation.

(4) Measured with f/1 optics.

PHILIPS LABORATORIES
DATA SHEET

PEV No.: 335A
Gun No.: 42479
Target : DTGFB, reticulated

ELECTRICAL

Filament	6.3 V	
G_2/G_3	280 V	0.8 µA
G_4	450 V	1.8 µA
Target	- 16.7 V	
Auxiliary Heater(1)	5.03 V	0.278 A
Alignment(2)	V = 1.88 mA	H = 3.17 mA
G_1 Forward	+ 8 V	
Cathode Forward	+ 2 V	
G_1 Reverse(3)	- 88 V	
Cathode Reverse(3)	- 92 V	

PERFORMANCE*

Lag(1) $\alpha = I/I_o = e^{-\beta} = 0.37$

$I_{pedestal}$ = 100 nA

* Scan 3:4 aspect ratio, 20 mm scan height.

	TVL/PH				
	10	50	100	150	200
Sensitivity(4) (nA/°C)	3.7	2.9	1.9	---	0.66
Contrast Transfer	1	0.78	0.51	---	0.18

Notes:

(1) Heater voltage set to achieve low spatial frequency sensitivity of 3.7 nA/°C. Volts may vary with camera conditions. Lag measured at S = 3.7 nA/°C.

(2) Alignment currents using Philips MP camera vidicon deflection coil.

(3) G_1 reverse is pulse voltage for pedestal generation.

(4) Measured with f/1 optics.

PHILIPS LABORATORIES
DATA SHEET

PEV No.: 333
Gun No.: 42387
Target : DTGFB, reticulated

ELECTRICAL

Filament	6.3 V	
G_2/G_3	280 V	2.5 µA
G_4	400 V	1.9 µA
Target	- 10 V	
Auxiliary Heater(1)	5.38 V	0.289 A
Alignment(2)	V = 1.29 mA	H = -0.25 mA
G_1 Forward	+ 9 V	
Cathode Forward	+ 2 V	
G_1 Reverse(3)	- 60 V	
Cathode Reverse(3)	- 68 V	

PERFORMANCE*

Lag(1) $\alpha = I/I_o = e^{-\beta} = 0.37$

$I_{pedestal} = 100$ nA

* Scan 3:4 aspect ratio, 20 mm scan height.

	TVL/PH				
	10	50	100	150	200
Sensitivity(4) (nA/°C)	3.0	2.5	1.82	---	0.78
Contrast Transfer	1	0.83	0.61	---	0.26

Notes:

(1) Heater voltage set to achieve low spatial frequency sensitivity of 3.0 nA/°C. Volts may vary with camera conditions. Lag measured at S = 3.0 nA/°C.

(2) Alignment currents using Philips MP camera vidicon deflection coil.

(3) G_1 reverse is pulse voltage for pedestal generation.

(4) Measured with f/1 optics.

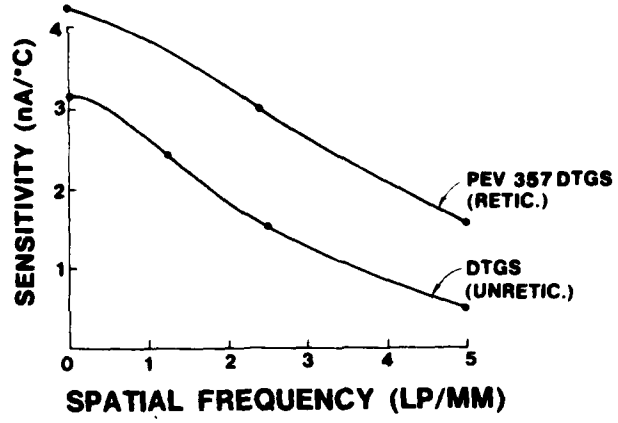

Figure 2. Signal vs. spatial frequency for PEV tube with reticulated DTGS.

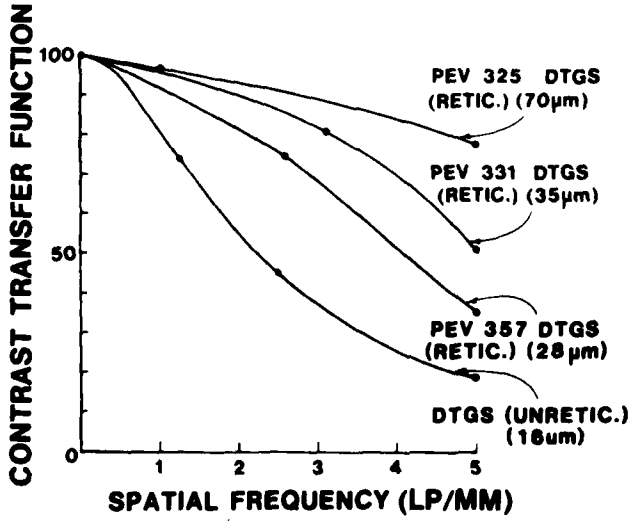

Figure 3. PEV tubes with reticulated DTGS.

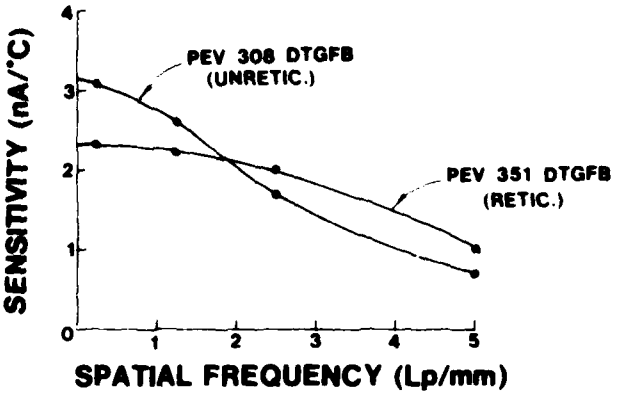

Figure 4. Signal vs. spatial frequency for PEV tube with reticulated DTGFB.

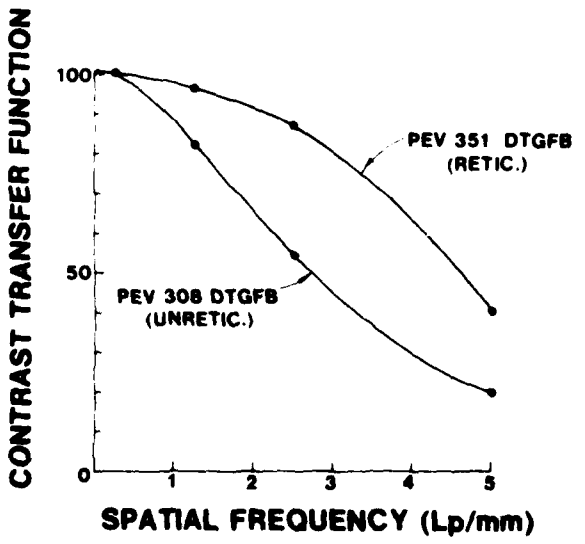

Figure 5. PEV tubes with reticulated DTGFB.

DISTRIBUTION LIST

1. Texas Instruments
   13500 N. Central Expressway
   Dallas, Texas 75222

2. Honeywell, Inc.
   Corporate Research Center
   Hopkins, Minnesota 55343

3. Barnes Engineering
   30 Commerce Road
   Stamford, Conn. 06902
   ATTN: R. Astheimer

4. R.C.A.
   Government and Commercial Systems
   1901 N. Moore Street
   Arlington, VA 22209
   ATTN: D. Reid

5. Westinghouse Corporation
   Defense and Space Center
   P.O. Box 1521
   Baltimore, MD 21203

6. ITT
   Electron Tube Division
   3700 E. Pontiac Street
   Fort Wayne, Indiana 46803
   ATTN: E. Eberhart

7. General Electric Company
   777 Fourteenth Street, N.W.
   Washington, D.C. 20005
   ATTN: D. Hunter

8. Hughes Aircraft Company
   Industrial Products Division
   2020 Oceanside Blvd.
   Oceanside, CA 92054
   ATTN: J. Koda

9. Inrad Corporation
   406 Paulding Drive
   Northvale, New Jersey 07647
   ATTN: Dr. W. Ruderman

10. Teltron Inc.
    Baltic Mews Industrial Park
    2 Riga Lane
    P.O. Box 416
    Douglassville, PA 19518
    ATTN: A. Mengel

11. Systems Research Laboratories Inc.
    2800 Indian Ripple Road
    Dayton, Ohio 45440
    ATTN: R. Holmes

12. Lockheed Missles & Space Inc.
    1111 Lockheed Way
    Sunnyvale, CA 94088

13. U.S. Naval Weapons Center
    China Lake, CA
    ATTN: W. Woodworth

END

DATE
FILMED

1-81

DTIC